Original papers

Arsenic trioxide induces the differentiation of retinoic acid-resistant neuroblastoma cells via upregulation of *HoxC9*

Chunmou Li[1,B–D], Chuchu Feng[1,B,D], Yantao Chen[2,B,C], Pingping Wu[1,B,D],
Peng Li[3,B,C], Xilin Xiong[1,B,C], Xiaomin Peng[1,B], Zhixuan Wang[1,C], Yang Li[1,A,E,F]

[1] Pediatric Hematology/Oncology, Children's Medical Center, Sun Yat-Sen Memorial Hospital, Sun Yat-Sen University, Guangzhou, China

[2] Department of Orthopaedics, Sun Yat-Sen Memorial Hospital, Sun Yat-Sen University, Guangzhou, China

[3] Key Laboratory of Regenerative Biology, South China Institute for Stem Cell Biology and Regenerative Medicine,
 Guangzhou Institutes of Biomedicine and Health, Chinese Academy of Sciences, China

A – research concept and design; B – collection and/or assembly of data; C – data analysis and interpretation;
D – writing the article; E – critical revision of the article; F – final approval of the article

Address for correspondence
Yang Li
E-mail: drliyang@126.com

Conflict of interest
None declared

Abstract

Background. Neuroblastoma (NB) is one of the most common extracranial tumors with limited therapeutic options. Retinoic acid (RA) has been identified to play anticancer role against NB cells by inducing the differentiation and apoptosis of immature neuroblasts. However, silencing *HoxC9* promoter by *EZH2*-induced H3K27me3 hypermethylation can lead to RA resistance. Previous studies have suggested that arsenic trioxide (ATO), an inhibitor of DNA methylation, could downregulate the expression of *EZH2* in breast cancer cells.

Objectives. In our study, we attempted to obtain some insight into the mechanisms of differentiation of RA-resistant NB cells by detecting the expressions of *HoxC9* and *EZH2* in NB cells treated with ATO, so as to provide a basis for the subsequent treatment of RA-resistant NB by ATO.

Materials and methods. Two NB cell lines, SK-N-AS (retinoic acid-resistant neuroblastoma cells) and SK-N-SH (retinoic acid-sensitive neuroblastoma cells), were used in our experiments. Cell proliferation and apoptosis were respectively determined with Cell Counting Kit-8 (CCK-8) assay kit and Annexin V staining. The inverted phase contrast microscope was used to observe cell growth and measure the total length of nerve synapses. We employed label-free quantitative proteomic analysis to profile ATO-dependent changes in the proteome of NB cells. Western blot was used to detect the expressions of *HoxC9*, *HoxD8* and *EZH2*.

Results. Arsenic trioxide inhibited the cell proliferation and increased apoptosis and total length of synapses in two NB cell lines. The expressions of *HoxC9* and *HoxD8* were upregulated, while the expression of *EZH2* was downregulated in the SK-N-AS cell line. No significant changes in the 3 proteins mentioned above were observed in the SK-N-SH cell line after ATO treatment.

Conclusions. Arsenic trioxide may reactivate the expression of *HoxC9* by downregulating *EZH2*, which leads to restoring RA sensitivity and promoting the differentiation and apoptosis of RA-resistant NB cells.

Key words: neuroblastoma, arsenic trioxide, retinoic acid resistance, *EZH2* gene, *HoxC9* promoter

Background

Neuroblastoma (NB), which results from the improper differentiation of neural crest progenitors, is the 2nd most frequent extracranial pediatric cancer,[1] accounting for about 10% of all malignancies in children and 15% of all cancer-related deaths in this population.[2,3] Although new treatment options constantly emerge over the past years, the long-term overall survival (OS) of high-risk NB is still below 50%.[4]

Retinoic acid (RA) can modulate the expression of its target genes in order to regulate the differentiation, apoptosis and proliferation in numerous types of cells.[5,6] As an effective inducer of cell differentiation, RA has been used for the treatment of high-risk NB.[7,8] Thus, RA-resistant NB may significantly contribute to minimal residual disease during RA maintenance therapy, even with more than 50% of the patients developing recurrent disease.[9] Patients with relapsed or refractory NB have, in general, poor prognosis and more than 60% of them will eventually die due to deteriorating health conditions within a few years.[10,11]

Homeobox (Hox) genes are well known for their ability to regulate embryogenesis and induce tissue differentiation.[12] It is currently assumed that HoxC9 can activate the intrinsic pathway of apoptosis and is associated with spontaneous regression in NB.[13,14] The expression of HoxC9-induced genes can significantly downregulate the oncogenic marker paired-like homeobox 2b (PHOX2B) in BE(2)-C and other NB cells, and upregulate the neuronal differentiation markers, like neurofilament medium (NEFM) and microtubule-associated protein 2 (MAP2).[14] The NEFM has been confirmed to be the target gene of HoxC9, and HoxC9 was confirmed to be a direct target gene of HoxD8.[14,15] However, to the best of our knowledge, the expression of Hox genes was not observed in RA-resistant NB cells during retinoic acid-therapy.[14] In addition, zeste homolog 2 (EZH2), as a methyltransferase, can extend gene silencing of Hox genes by trimethylating histone H3 lysine 27 (H3K27me3) in NB cells.[16–18]

Arsenic trioxide (ATO) is an ancient drug from China which currently entered the clinical arena as a Food and Drug Administration (FDA)-approved drug for the treatment of acute promyelocytic leukemia (APL).[19,20] One study has suggested that ATO could significantly upregulate HoxB8 in both mRNA and protein levels during hematopoietic stem cell (HSC) differentiation into the colony forming unit-granulocyte (CFU-G).[21] As a methylation inhibitor, ATO could also provoke the expression or reactivation of tumor suppressor genes (GSTP1, RASSF1A, etc.) with CpG islands demethylation by suppressing DNA methyltransferases (DNMT) in liver cancer.[22]

Objectives

In our study, we detected the expressions of Hox genes and EZH2 in RA-resistant NB cells to elucidate whether ATO could reactivate the expression of HoxC9 by downregulating EZH2, leading to the restoration of RA sensitivity and promotion of the differentiation and apoptosis of RA-resistant NB cells. With this experimental setup, we attempt to provide a novel therapeutic intervention for NB patients with RA-resistant feature.

Materials and methods

Materials

Dulbecco's modified Eagle's medium (DMEM) and heat-inactivated fetal bovine serum (FBS) were purchased from Gibco (Waltham, USA). Arsenic trioxide was purchased from Harbin Yida Pharmaceutical Co., Ltd. (Harbin, China). Cell Counting Kit-8 Assay (CCK-8) was purchased from APExBIO (Houston, USA). Annexin V-FITC Apoptosis Detection Kit (Annexin V-FITC/PI) was purchased from Beyotime Biotechnology (Beijing, China). The BCA kit was purchased from Beyotime Biotechnology. Anti-HoxC9, anti-HoxD8 and anti-EZH21 antibodies were purchased from Abcam (Cambridge, UK). The horseradish peroxidase (HRP)-linked whole antibody anti-mouse immunoglobulin G (IgG) was purchased from Cell Signaling Technology (CST, Darmstadt, Germany). The protein markers were purchased from Thermo Fisher Scientific (Waltham, USA). The Click-it EdU Alexa Fluor 488 Flow Cytometry Assay was purchased from Invitrogen (Waltham, USA). All procedures were performed according to the manufacturers' protocols.

Cell cultures

For this study, we chose 2 human NB cell lines for culture: SK-N-AS (retinoic acid-resistant neuroblastoma cells) and SK-N-SH (retinoic acid-sensitive neuroblastoma cells), both obtained from the Sun Yat-Sen University (Guangzhou, China). Cell line authentication to confirm genomic identity was performed and the continual tests of mycoplasma contamination were run after each thaw. Both cell lines were cultured in DMEM (with 10% FBS and 1% penicillin-streptomycin) at 37°C in a 5% CO_2 incubator. After growing as a monolayer and multilayers with 70−80% confluence in T75 cell culture flasks with 15 mL of media, the cells were adjusted at a density of 1×10^4/mL and then transferred to a 96-well plate.

Cytotoxicity assay

The CCK-8 assay was used to detect cell cytotoxicity. Both cell lines were seeded in 96-well plates with 1000 cells (1×10^4/mL; 100 µL) per well separately. Arsenic trioxide treatment was performed in triplicate 24 h later. Based on our previous experience, the 50% inhibitory concentration of ATO ($IC50_{ATO}$) value of NB cells was set at 2–128 µM for 24 h. Thus, we chose the ATO

concentrations of 1–256 µM for this experiment. The cells, drugs, medium, and CCK-8 reagent were contained in experimental wells; control wells set with the cells, medium and CCK-8 reagent; blank control contained no cells. After incubation for 60 min in the dark, the optical density (OD) value was measured at a 450 nm wavelength using a microplate reader (SpectraMax Plus 384; Molecular Devices, Sunnyvale, USA), and the relative viability was calculated as follows:

the relative viability = [(experimental absorbance – background absorbance)/(untreated control absorbance – background absorbance)] × 100%.

In our experiment, to assess the effect of ATO on NB cells differentiation, the synaptic growth was chosen as a representative feature. After both cell lines were cultured with ATO for 24 h in IC50 (95.36 µM in SK-N-AS, 5.52 µM in SK-N-SH), apoptotic NB cells became round and suspended. Thus, we reduced the concentration of ATO and tried to find a proper one in order to obtain a better observation result of synapses. To achieve this purpose, we cultured them with their $^1/_2$ IC50 (48 µM in SK-N-AS cells, 2.7 µM in SK-N-SH cells), $^1/_3$ IC50 (32 µM in SK-N-AS, 1.9 µM in SK-N-SH), $^1/_6$ IC50 (16 µM in SK-N-AS, 0.9 µM in SK-N-SH), and $^1/_{12}$ IC50 (8 µM in SK-N-AS, 0.5 µM in SK-N-SH) concentrations to find out the optimal one by comparison.

Cell morphology

Both cell lines in the logarithmic growth phase were seeded in 6-well microplates (6×10^5 cells/well) as a single-cell suspension and cultured for 24 h to attach to the plate. Then, they were treated with or without ATO and grown in DMEM with 10% FBS and 1% penicillin-streptomycin for 24 h at 37°C in a 5% CO_2 cell culture incubator (HERA Cell 240i; Thermo Fisher Scientific). To avoid the interference of apoptosis on the observation of differentiation, by comparison, $^1/_6$ IC50 concentration (16 µM) of SK-N-AS cells and $^1/_2$ IC50 concentration (2.7 µM) of SK-N-SH cells were chosen for observation of cell morphology. After 24-hour treatment with or without ATO (the cells were adherent to walls at this time), we used inverted phase contrast microscopy (DP50 digital camera; Olympus Corp., Tokyo, Japan) to evaluate the cellular morphological changes. The length of neurites was tallied using the ImageJ program v. 1.51 (National Institutes of Health (NIH), Bethesda, USA) with the assistance of the NeuronJ Plugin, which can provide semi-automated tracing.

Apoptosis assay

We used flow cytometry (FCM) assay purchased from Invitrogen to conduct the apoptosis assay. The experiment was carried out in accordance with the manufacturer's instructions. After the treatment with ATO, trypsinization was used to harvest the cells, which were then collected by centrifugation at 1000 rpm for 5 min. The cells were rinsed in PBS once more before the collection by centrifugation.

The both collected cell lines were suspended in 400 uL Ca^{2+} Binding Buffer (Abcam) and split equally into 2 tubes. One tube was supplemented with 5 µL of fluorescein isothiocyanate (FITC) reagents, and the other one was used as a blank control group without any treatment. Then, 10 µL of propidium iodide (PI) dyes were applied to each sample and the samples were incubated at room temperature for 15 min in the dark.

Two different markers (FITC conjugated to Annexin V as an apoptotic cell marker and PI as a dead cell marker) were contained in Annexin V-FITC/PI Apoptosis Detection Assay Kit (Invitrogen). In this test, the ratio of fluorescence intensities excited at 488 nm was monitored at an emission wavelength of 515 nm for FITC and 560 nm for PI. Apoptotic cells were collected and at least 10,000 cells were counted for all FCM experiments to ensure the accuracy. The experiment was repeated in triplicate.

Phosphoproteomic analysis

Both cell lines in the logarithmic growth phase were processed to single-cell suspension and cultured in 15-centimeter cell culture dishes (2×10^6/mL, 20 mL). Cells were incubated using the method described in the cell morphology subsection. After the cells adhered to the walls of the dishes, they were treated with or without ATO for 24 h, and then collected for measuring protein abundances with mass spectroscopy analysis at PTM Biolabs, Inc. (Hangzhou, China).

Protein extraction

All operations were carried out on ice. The cells were sonicated 3 times with a high-intensity ultrasonic processor (SCIENTZ-1200E; Ningbo Scientz Biotechnology Co., Ltd., Ningbo, China) in lysis buffer (8 M urea and 1% Protease Inhibitor Cocktail; Roche, Basel, Switzerland). The supernatant was collected after centrifugation at 12,000 × g for 10 min at 4°C (in order to remove the residual debris). The BCA kit was then used to determine the protein content.

Trypsin digestion

The protein solution was alkylated with 11 mM iodoacetamide for 15 min at room temperature in darkness after being reduced with 5 mM dithiothreitol for 30 min at 56°C. The protein sample was then diluted with 100 mM triethylammonium bicarbonate (TEAB) to achieve a lower urea content (less than 2 M). Following the aforementioned process, trypsin was introduced at a 1:50 trypsin-to-protein mass ratio for the 1st overnight digestion, and a 1:100 trypsin-to-protein mass ratio for the 2nd 4-hour digestion.

906

C. Li et al. ATO induces the differentiation of NB cells

Mass spectroscopy analysis

The tryptic peptides were separated using an EASY-nLC 1000 UPLC machine (Thermo Fisher Scientific) after being dissolved in 0.1 percent formic acid (solvent A; Thermo Fisher Scientific). The peptides were evaluated using tandem mass spectroscopy (MS) in Q Exactive™ Plus mass spectrometer (Thermo Fisher Scientific) linked online to the ultra-performance liquid chromatography (UPLC) with the nanospray ionization source. The pieces were identified in the Orbitrap (Thermo Fisher Scientific) at 17,500 resolutions using a normalized collision energy value of 28 for UPLC-tandem mass spectrometry (UPLC-MS/MS). One MS scan was followed by 20 MS/MS scans with 15.0 s dynamic exclusion in a data-dependent method. Automatic gain control (AGC) was set to 5E4 (automatic gain control); 100 m/z was chosen as the fixed initial mass.

Database search

The MS/MS data were analyzed using the Maxquant search engine v. 1.5.2.8 (https://www.maxquant.org/). Tandem mass spectra were compared to the Uniprot Human database (https://www.uniprot.org/), which was combined with the reverse decoy database (unip_Anas_8839 database). Trypsin/P was chosen as the cleavage enzyme, allowing for up to 4 missed cleavages. The mass tolerance for precursor ions was set to 20 ppm in the First search and 5 ppm in the Main search. Additionally, the mass tolerance for fragment ions was set to 0.02 Da. Carbamidomethylation on cysteine (Cys) was designated as a fixed modification, whereas acetylation and oxidation on methionine (Met) were designated as variable modifications. False discovery rate (FDR) was adjusted to <1% and a score greater than 40 was set for modified peptides.

Bioinformatics methods

The Gene Ontology (GO) annotation covers cellular composition (CC), molecular function (MF) and biological process (BP), and it is applied for bioinformatics analysis by evaluating differentially expressed genes (DEGs) and associated gene modules, based on the substantial enrichment of GO functions. The UniProt-GOA database (http://www.ebi.ac.uk/GOA/) was used for the GO annotation proteome by identifying protein IDs, converting them to UniProt IDs, and then mapping them to GO IDs by protein ID. If any of the proteins were not annotated by the UniProt-GOA database, the InterProScan online software (http://www.ebi.ac.uk/InterProScan/) was used as a substitute method based on protein sequence alignment technique.

Western blot

Whole-cell lysates from both cell lines (with or without ATO) were investigated using standard western blotting techniques. Both cell lines were seeded in 6-well microplates (6×105 cells/well) as a single-cell suspension and cultured for 24 h. After the cells adhered to the walls of the plates and were treated with or without ATO for 24 h, 2–3 mL of precooled PBS were added to wash the cells, and then the samples were immediately placed on ice. After that, 100 μL of lysate was added for 30 min in order to achieve full lysis. Protein lysates were denatured at 95°C for 5 min after being collected and centrifuged (1200 r/min, 4°C) for 5 min, and then they were stored at −80°C. Protein concentration was measured using BCA protein assay. The absorbance was measured with enzyme labeling instrument at 592 nm wavelength, and concentration of each sample was calculated based on standard curve analysis. Approximately 20 μg of protein were run on 4–15% gradient Tris-Glycine Gels (Thermo Fisher Scientific). Before being transferred with the Trans-Blot Turbo transfer system (Bio-Rad, Hercules, USA), the concentrated gel was run at 80 V and separation gel at 120 V constant pressure electrophoresis. After blocking the membranes for 1 h at room temperature with 5% skim milk powder, the membranes were incubated with the 1st antibody (1:1000) in Tris-buffered saline containing 0.1% Tween20 (TBST) overnight at 4°C. The membrane was washed 3 times with TBST, incubated for 1 h with the 2nd antibody of HRP-labeled anti-mouse IgG (1:2000), and rinsed 3 times with TBST before using electrochemiluminescence (ECL) reagent to visualize the blots. A gel documentation system (Biozym, Hessisch Oldendorf, Germany) was applied to quantify the scanned film, following gel electrophoresis.

Statistical analyses

We used IBM SPSS v. 25.0 (IBM Corp., Armonk, USA) and GraphPad Prism software v. 8.0 (GraphPad Software, San Diego, USA) to analyze the data. Before applying parametric statistics, we used Levene's test for the homogeneity of variance and Kolmogorov–Smirnov tests combined with QQ-plots for the normality of data. If the quantitative data fulfilled the necessary conditions, the Student's t-test was used. The rank-sum test was performed if the normal distribution or the homogeneity of the variance was not met. Values of $p < 0.0500$ were considered to indicate statistically significant differences. The IC50 values are not cases of simple linear regression, but they reflect nonlinear parameter optimization and fit using a sigmoidal dose-response model. In our experiment, a 4-parameter logistic equation was employed using Microsoft Excel 2019 (Microsoft Corp., Redmond, USA) and GraphPad Prism for curve fitting analysis to determine IC50 values.

Results

SK-N-AS and SK-N-SH cells growth inhibition with different concentration of ATO

In order to evaluate the cytotoxicity of ATO, both SK-N-AS and SK-N-SH cells were seeded in 96-well cell culture plates with 1000 cells (1×10^4/mL; 100 µL) per well separately and treated with different concentration of ATO ranging from 1 µM to 2^8 µM. The CCK-8 assay was used to detect cell cytotoxicity. In SK-N-AS cells, the inhibition rate (mean ± standard deviation (SD)) was 1.1 ±5.1%, 8.5 ±0.7%, 17.1 ±4.5%, 25.9 ±0.2%, 37.5 ±2.1%, 44 ±1.0%, 48.3 ±1.9%, 48.9 ±0.9%, and 55.9 ±0.8% in different ATO concentrations (1 µM, 2 µM, 4 µM, 8 µM, 16 µM, 32 µM, 64 µM, 128 µM, and 256 µM) at 24 h. The inhibition rate of proliferation markedly elevated from 4 µM to 128 µM and plateaued thereafter (Fig. 1). The $IC50_{ATO}$ value of SK-N-AS cells was 95.36 µM at 24 h, calculated with Graph-Pad Prism. The $IC50_{ATO}$ value (5.52 µM) of SK-N-SH cells was obtained the same way as above (Fig. 1), which corresponded with our previous experimental results.[23] To avoid
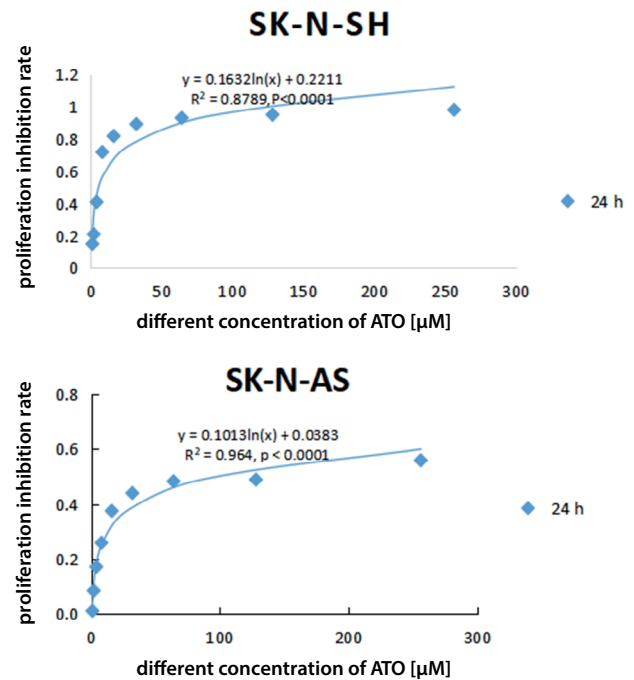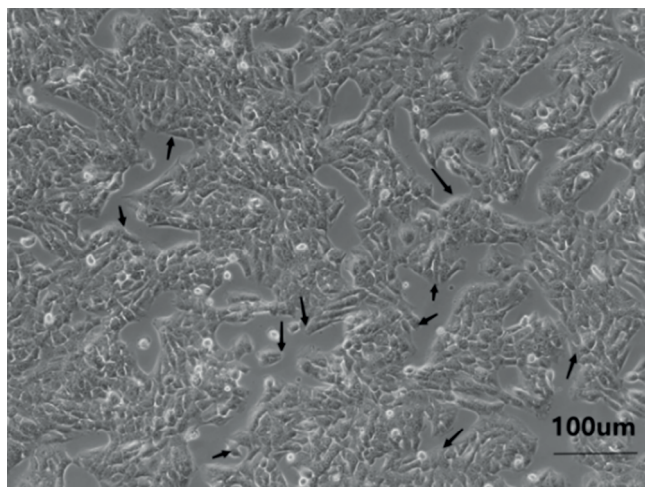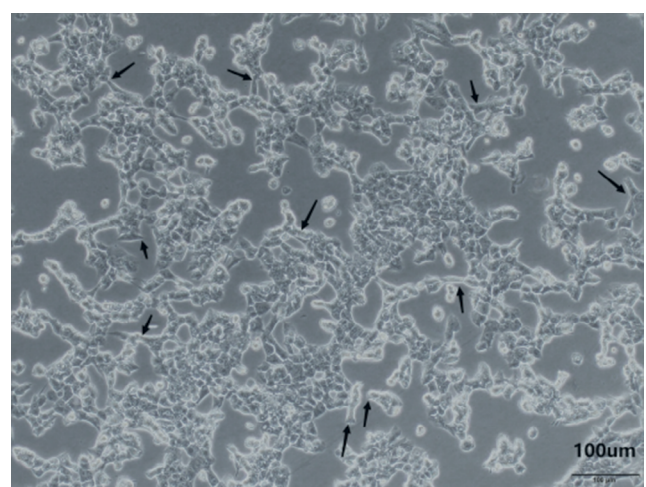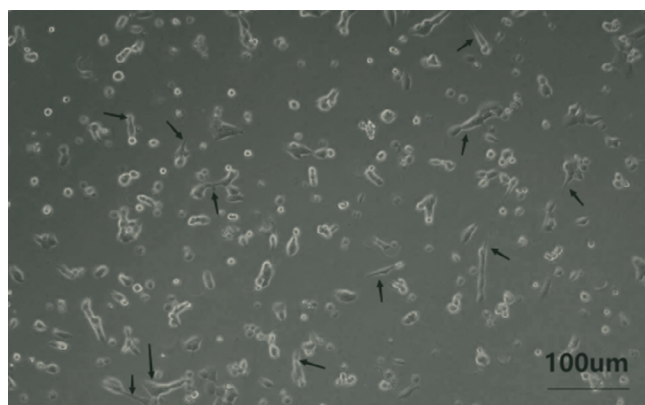

Fig. 1. Proliferation inhibition rate of SK-N-AS (retinoic acid-resistant neuroblastoma) and SK-N-SH (retinoic acid-sensitive neuroblastoma) cells with different concentration of arsenic trioxide (ATO) at 24 h
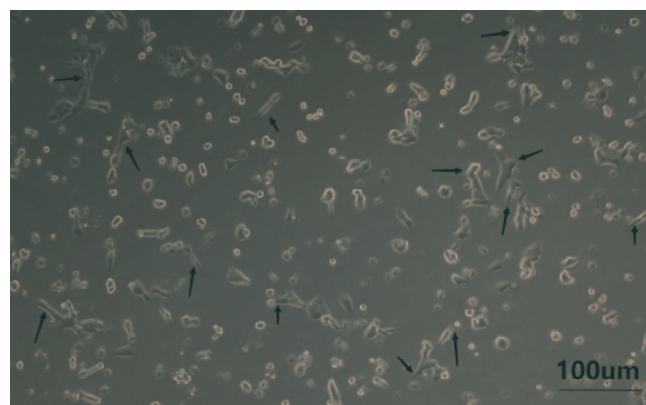

The control group of SK-N-AS (without ATO)

The experimental group of SK-N-AS (with ATO)

The control group of SK-N-SH (without ATO)

The experimental group of SK-N-SH (with ATO)

Fig. 2. Cell morphology of SK-N-AS (retinoic acid-resistant neuroblastoma) and SK-N-SH (retinoic acid-sensitive neuroblastoma) cells with or without arsenic trioxide (ATO)

the interference of apoptosis on the observation of differentiation, by comparison, $^1/_6$ IC50 concentration (16 µM) of SK-N-AS cells and $^1/_2$ IC50 concentration (2.7 µM) of SK-N-SH cells were chosen for observation of cell morphology, apoptosis assay, phosphoproteomic analysis, and western blot.

ATO accelerated synaptic growth of SK-N-AS and SK-N-SH cells

To assess the effect of ATO on NB cells differentiation, the synaptic growth was chosen as a representative feature (longer synaptic represents better differentiation). We cultured both cell lines with or without ATO for 24 h, and more synapses in 2 cell lines were observed in the experimental group (with ATO) than the control group (without ATO) using inverted phase contrast microscopy (Fig. 2). In both cell lines, using ImageJ program with NeuronJ Plugin, we found that the length of synapses (1 field was randomly selected under microscope with ×100 magnification) grew longer with time in culture in both cells, and the total length of synapses in the experimental group significantly increased compared to the control group (Table 1,2). We can conclude that ATO could morphologically promote the differentiation of NB cells.

ATO promoted apoptosis of SK-N-AS and SK-N-SH cells

We cultured both cell lines with or without ATO for 24 h and the apoptotic rates of the 2 groups were analyzed with FCM. Results were expressed as mean ±SD. We found that the apoptotic rate of SK-N-AS cells in the experimental group was significantly higher (Fig. 3)
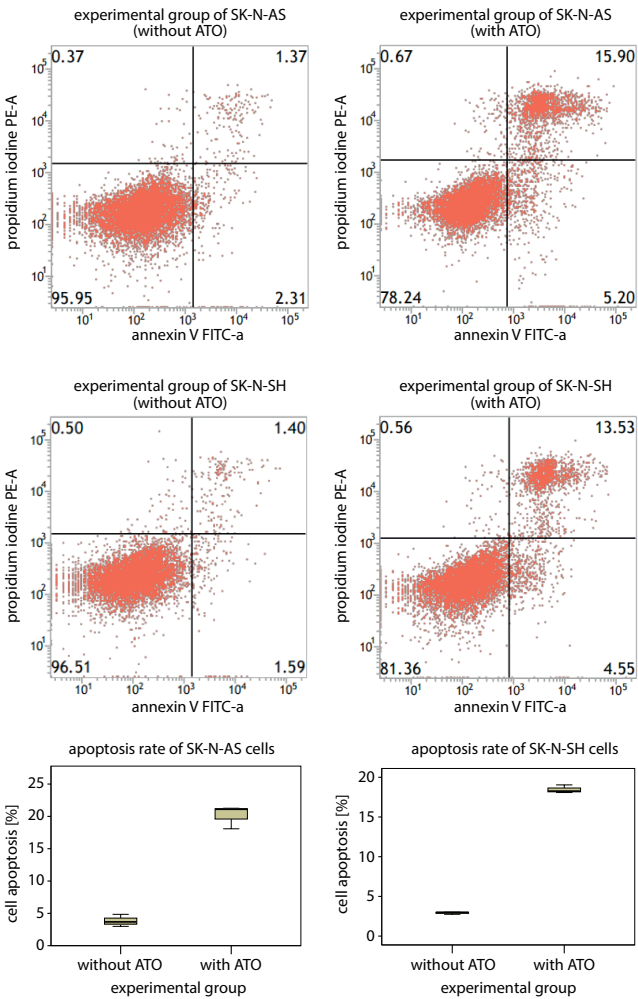

Fig. 3. The apoptosis rate of SK-N-AS (retinoic acid-resistant neuroblastoma) and SK-N-SH (retinoic acid-sensitive neuroblastoma) cells with or without arsenic trioxide (ATO)

than that in the control group (20.15 ±1.79% compared to 3.84 ±0.94%, p < 0.0001). In SK-N-SH cells, a significant increase of apoptosis could also be observed in the experimental group compared to the control group.

Different intracellular protein expressions between the experimental group and control group of SK-N-AS and SK-N-SH cells

In order to figure out the different intracellular protein expressions before and after the treatment with ATO,

Table 1. Total lengths of synapses of SK-N-AS and SK-N-SH cells with or without ATO

| Time [h] | Total lengths of synapses [µM] | | | |
| | control group (without ATO) | | experimental group (with ATO) | |
	SK-N-AS	SK-N-SH	SK-N-AS	SK-N-SH
0	0	0	0	0
24	96	84	723	435

Table 2. The p-value of normality test and homogeneity test

| Group | Total lengths of synapses | | Apoptosis rate | |
	normality	homogeneity	normality	homogeneity
Control group (without ATO) of SK-N-AS cells	0.826	0.050	0.718	0.050
Experimental group (with ATO) of SK-N-AS cells	0.126		0.085	
Control group (without ATO) of SK-N-SH cells	0.157	0.050	1.000	0.050
Experimental group (with ATO) of SK-N-SH cells	0.194		0.680	

ATO – arsenic trioxide; SK-N-AS – retinoic acid-resistant neuroblastoma cells; SK-N-SH – retinoic acid-sensitive neuroblastoma cells.

we compared intracellular protein expressions of SK-N-AS and SK-N-SH cells between the experimental group (with ATO) and control group (without ATO). We identified quantitative information for 6424 proteins in the SK-N-AS cell line and 4638 proteins in the SK-N-SH cell line. Differentially expressed protein (DEP) was identified by comparison of the signal values between the 2 groups based on $p < 0.05$ using t-test. In SK-N-AS cells, we identified that the neuronal markers MAPT and NEFM were upregulated, and the tumorigenic marker PHOX2B were downregulated in the ATO-treated group. As compared with the control group, we found that EZH2 (FC = 0.552) and PHOX2B (an oncogenic marker, FC = 0.142) were significantly downregulated, while the markers related to the normal differentiation of neurons were upregulated, like MAPT (FC = 1.21), NEFM (FC = 1.547) and MAP2 (FC = 2.669) in the experimental group. In SK-N-SH cells, the same changing trends of the markers mentioned above (PHOX2B was not detected in SK-N-SH cells), but the disparity coefficients of most proteins were smaller than in the SK-N-AS cells, such as for EZH2 (FC = 0.691), MAPT (FC = 1.312), NEFM (FC = 1.146), MAP2 (FC = 1.086), and others. We tested the protein expressions of HoxC9, HoxD8 and EZH2 in SK-N-AS with or without ATO using western blot. We found that, compared to control group, ATO could upregulate HoxC9 and HoxD8, and downregulate EZH2 (Fig. 4,5).
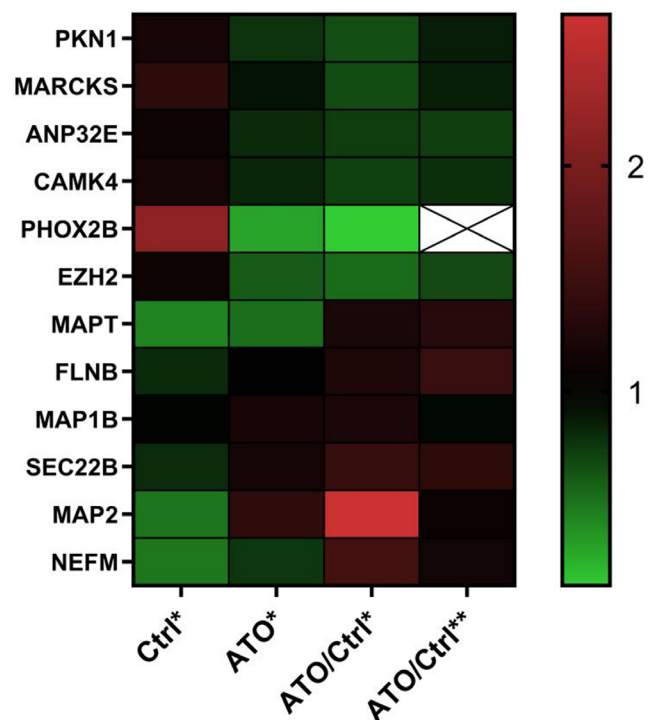

Fig. 4. Differential protein expressions in both cell lines (heat map)

Ctrl* – the control group (without ATO) in the SK-N-AS (retinoic acid-resistant neuroblastoma) cells; ATO* – the experimental group (with ATO) in the SK-N-AS cells; ATO/Ctrl* – ratio of protein expression in the experimental group to the control group in the SK-N-AS (retinoic acid-sensitive neuroblastoma) cells; ATO/Ctrl** – ratio of protein expression in the experimental group to the control group in the SK-N-SH cells; ATO – arsenic trioxide.

Discussion

The NB, which derives from embryonic neural crest, has self-renewable capacities and can differentiate multidirectionally during dorsal migration from the neural tube to the ventral side.[23] When neuroblasts fail to migrate correctly and remain undifferentiated, NB occurs.[24] The degree of differentiation is assessed by the total neurite length, co-expression of neurofilament and synaptic vesicles, and shape of the cone.[25] Notably, total neurite length is directly involved in the neural differentiation.[26,27] The MAP2,
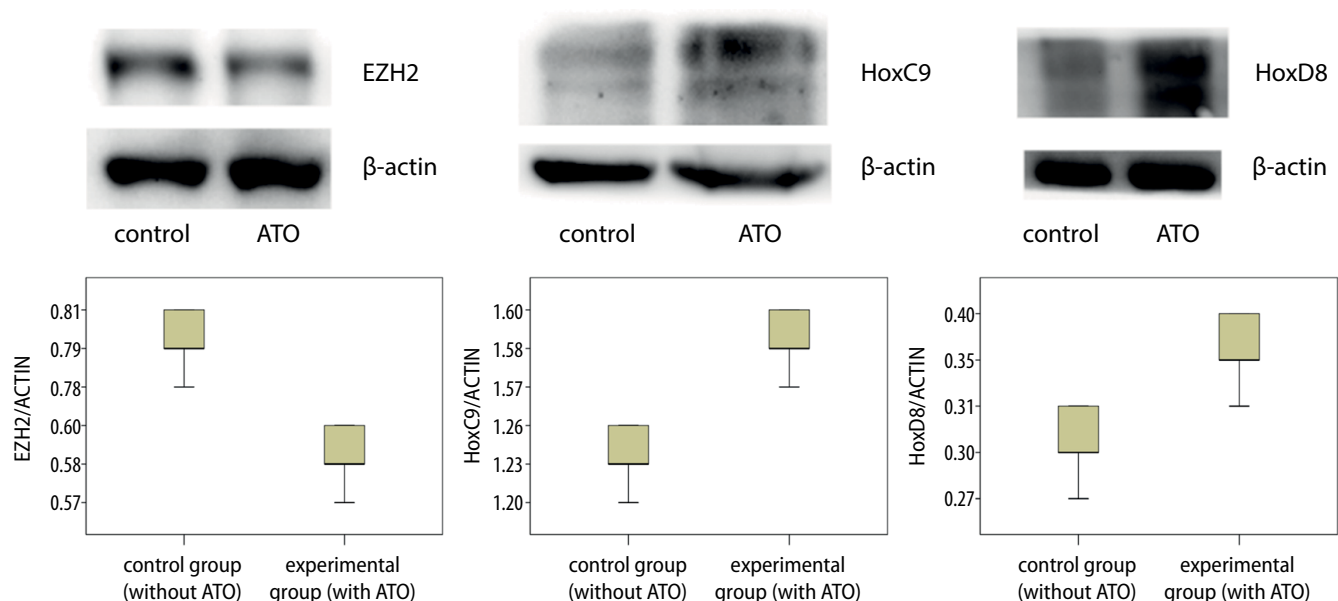

Fig. 5. Different protein expressions of HoxC9, HoxD8 and EZH2 in SK-N-AS (retinoic acid-resistant neuroblastoma) cells with arsenic trioxide (ATO)

as a neuronal differentiation marker, can maintain neuronal dendritic spines by interacting with microtubules.[28] It has been reported that the expression of MAP2 could be upregulated by RA through brain-derived neurotrophic factor (BDNF) in SH-SY5Y cells.[29,30] A study on whole genome sequencing of fetal adrenal cells has found that PHOX2B is a marker of sympathetic progenitors, which is significantly downregulated during the differentiation process of sympathetic nerves.[31] The NEFM gene encodes a subunit of neuron-specific intermediate filaments[32]; its expression was reduced after ATO administration.[33] The NEFM was verified to be the target of RA in NB cells, as well as the direct target of HoxC9.[7] Our study verified that expressions of HoxC9 and HoxD8 in SK-N-AS cells were upregulated. Label-free quantitative proteomic technology identified that tumorigenic marker PHOX2B was significantly downregulated, while the markers for differentiation of sympathetic neurons (NEFM, MAP2, MAPT) were upregulated. Similarly to the results of previous studies, the expressions of NEFM, MAP2 and MAPT were decreased after RA treatment in SH-SY5Y cells.[34] The above results suggest that low doses of ATO could reprogram RA-resistant NB cells differentiation, which may be due to the upregulation of HoxC9. In SK-N-SH cell line, the same changing trends of the markers mentioned above, except PHOX2B, HoxC9 and HoxD8 (not detected), were observed after ATO treatment, but the disparity coefficients of most proteins were smaller compared to the SK-N-AS cell line. However, in our view, this phenomenon can be explained. The SK-N-SH cell line, with RA-sensitive feature, might not possess the inhibition of HoxC9 pathway, and thus ATO could not ameliorate the differentiation by the mechanism of enhancing HoxC9 (via disinhibition). The H3K27me3 is a repressive histone mark, frequently seen in various kinds of tumors and associated with poor prognosis.[35] The H3K4me3, a silencing marker of HoxC9 promoter, is represented in an activated state in RA-resistant NB cells and conversely silenced in RA-sensitive cell lines.[14] This may partly explain why RA could not induce the expression of HoxC9 in SK-N-AS cell line. The methylation of histone is catalyzed by 2 different families: the protein arginine methyltransferases (RMTs) and the histone lysine methyltransferases (KMTs). Among them, methyltransferase EZH2 is known to be closely associated with the tumorigenesis and tumor development.[36] Previous studies showed that histone deacetylase inhibitors (HDACi) targets EZH2 and SUZ12, which are the major components of the PRC2 complex, ultimately reducing the H3K27me3 methylation.[37,38]

Our phosphoproteomic analysis revealed that ATO downregulates the expression of EZH2 in both cell lines; western blotting also confirmed this result, accompanied by the overexpression of HoxC9 in SK-N-AS cells. Based on existing literature, we speculate that ATO may act through a mechanism similar to HDACi, which could reduce repressive H3K27me3 through downregulating the expression of EZH2, and then reactivate HoxC9.

Limitations

However, there are also some shortcomings of this experiment. First, only 2 human NB cell lines were chosen, which could affect the robustness of the results. Second, the results confirm that ATO could upregulate the expression of HoxC9 and enhance neuronal differentiation, but we did not confirm the direct relationship between HoxC9 and neuronal differentiation. Finally, we mentioned that ATO might reduce repressive H3K27me3 through downregulating the expression of EZH2, and then reactivate HoxC9, but methylation assays were not performed to confirm this result.

Conclusion

The ATO-mediated EZH2 suppression of RA-resistant NB cells induces HoxC9 expression that, in turn, ameliorates differentiation and enhances cell apoptosis. Further study is necessary to compensate for the abovementioned limitations and support our conclusion.

ORCID iDs

Chunmou Li ⓘ https://orcid.org/0000-0001-8279-5115
Chuchu Feng ⓘ https://orcid.org/0000-0002-0322-2544
Yantao Chen ⓘ https://orcid.org/0000-0001-9638-2661
Pingping Wu ⓘ https://orcid.org/0000-0002-1822-4294
Peng Li ⓘ https://orcid.org/0000-0003-4530-2400
Xilin Xiong ⓘ https://orcid.org/0000-0002-5634-0544
Xiaomin Peng ⓘ https://orcid.org/0000-0002-0376-9400
Zhixuan Wang ⓘ https://orcid.org/0000-0002-5721-8639
Yang Li ⓘ https://orcid.org/0000-0002-1756-5847

Reference

1. Halakos EG, Connell AJ, Glazewski L, Wei S, Mason RW. Bottom up proteomics reveals novel differentiation proteins in neuroblastoma cells treated with 13-cis retinoic acid. J Proteomics. 2019;209:103491. doi:10.1016/j.jprot.2019.103491
2. Maris JM, Hogarty MD, Bagatell R, Cohn SL. Neuroblastoma. Lancet. 2007;369(9579):2106–2120. doi:10.1016/S0140-6736(07)60983-0
3. Smith V, Foster J. High-risk neuroblastoma treatment review. Children. 2018;5(9):114. doi:10.3390/children5090114
4. Pinto NR, Applebaum MA, Volchenboum SL, et al. Advances in risk classification and treatment strategies for neuroblastoma. J Clin Oncol. 2015;33(27):3008–3017. doi:10.1200/JCO.2014.59.4648
5. Karapolat S, Sanli A, Onen A, Acikel U, Sivrikoz O. Effects of retinoic acid on compensatory lung growth. J Cardiothorac Surg. 2008;3(1):37. doi:10.1186/1749-8090-3-37
6. Theodosiou M, Laudet V, Schubert M. From carrot to clinic: An overview of the retinoic acid signaling pathway. Cell Mol Life Sci. 2010; 67(9):1423–1445. doi:10.1007/s00018-010-0268-z
7. Park JR, Eggert A, Caron H. Neuroblastoma: Biology, prognosis, and treatment. Hematol Oncol Clin North Am. 2010;24(1):65–86. doi:10.1016/j.hoc.2009.11.011
8. Volchenboum SL, Cohn SL. Progress in defining and treating high-risk neuroblastoma: Lessons from the bench and bedside. J Clin Oncol. 2009;27(7):1003–1004. doi:10.1200/JCO.2008.20.2739
9. Nguyen T, Hocker JE, Thomas W, et al. Combined RARα- and RXR-specific ligands overcome N-myc-associated retinoid resistance in neuroblastoma cells. Biochem Biophys Res Commun. 2003;302(3):462–468. doi:10.1016/S0006-291X(03)00177-3
10. Keshelava N, Davicioni E, Wan Z, et al. Histone deacetylase 1 gene expression and sensitization of multidrug-resistant neuroblastoma cell lines to cytotoxic agents by depsipeptide. J Natl Cancer Inst. 2007;99(14):1107–1119. doi:10.1093/jnci/djm044

11. Lau DT, Hesson LB, Norris MD, Marshall GM, Haber M, Ashton LJ. Prognostic significance of promoter DNA methylation in patients with childhood neuroblastoma. *Clin Cancer Res*. 2012;18(20):5690–5700. doi:10.1158/1078-0432.CCR-12-0294

12. Berletch JB, Deng X, Nguyen DK, Disteche CM. Female bias in Rhox6 and 9 regulation by the histone demethylase KDM6A. *PLoS Genet*. 2013;9(5):e1003489. doi:10.1371/journal.pgen.1003489

13. Kocak H, Ackermann S, Hero B, et al. Hox-C9 activates the intrinsic pathway of apoptosis and is associated with spontaneous regression in neuroblastoma. *Cell Death Dis*. 2013;4(4):e586–e586. doi:10.1038/cddis.2013.84

14. Mao L, Ding J, Zha Y, et al. HoxC9 links cell-cycle exit and neuronal differentiation and is a prognostic marker in neuroblastoma. *Cancer Res*. 2011;71(12):4314–4324. doi:10.1158/0008-5472.CAN-11-0051

15. Zha Y, Ding E, Yang L, et al. Functional dissection of HOXD cluster genes in regulation of neuroblastoma cell proliferation and differentiation. *PLoS One*. 2012;7(8):e40728. doi:10.1371/journal.pone.0040728

16. Wan C, Liu X, Bai B, Cao H, Li H, Zhang Q. Regulation of the expression of tumor necrosis factor related genes by abnormal histone H3K27 acetylation: Implications for neural tube defects. *Mol Med Rep*. 2018;17(6):8031–8038. doi:10.3892/mmr.2018.8900

17. Ziegler C, Finke J, Grüllich C. Features of cell death, mitochondrial activation and caspase dependence of rabbit anti-T-lymphocyte globulin signaling in lymphoblastic Jurkat cells are distinct from classical apoptosis signaling of CD95. *Leuk Lymphoma*. 2016;57(1):177–182. doi:10.3109/10428194.2015.1044449

18. Kanduri M, Sander B, Ntoufa S, et al. A key role for EZH2 in epigenetic silencing of HOX genes in mantle cell lymphoma. *Epigenetics*. 2013;8(12):1280–1288. doi:10.4161/epi.26546

19. Au WY, Li CK, Lee V, et al. Oral arsenic trioxide for relapsed acute promyelocytic leukemia in pediatric patients. *Pediatr Blood Cancer*. 2012;58(4):630–632. doi:10.1002/pbc.23306

20. Iland HJ, Bradstock K, Supple SG, et al. All-trans-retinoic acid, idarubicin, and IV arsenic trioxide as initial therapy in acute promyelocytic leukemia (APML4). *Blood*. 2012;120(8):1570–1580. doi:10.1182/blood-2012-02-410746

21. Liu WJ, Jiang NJ, Guo QL, Xu Q. ATRA and As_2O_3 regulate differentiation of human hematopoietic stem cells into granulocyte progenitor via alteration of HoxB8 expression. *Eur Rev Med Pharmacol Sci*. 2015;19(6):1055–1062. PMID:25855932.

22. Cui X, Wakai T, Shirai Y, Yokoyama N, Hatakeyama K, Hirano S. Arsenic trioxide inhibits DNA methyltransferase and restores methylation-silenced genes in human liver cancer cells. *Hum Pathol*. 2006;37(3):298–311. doi:10.1016/j.humpath.2005.10.013

23. Qi K, Li Y, Huang K, et al. Pre-application of arsenic trioxide may potentiate cytotoxic effects of vinorelbine/docetaxel on neuroblastoma SK-N-SH cells. *Biomed Pharmacother*. 2019;113:108665. doi:10.1016/j.biopha.2019.108665

24. Palacios-Moreno J, Foltz L, Guo A, et al. George L neuroblastoma tyrosine kinase signaling networks involve FYN and LYN in endosomes and lipid rafts. *PLoS Comput Biol*. 2015;11(4):e1004130. doi:10.1371/journal.pcbi.1004130

25. Anitha M, Shahnavaz N, Qayed E, et al. BMP2 promotes differentiation of nitrergic and catecholaminergic enteric neurons through a Smad1-dependent pathway. *Am J Physiol Gastrointest Liver Physiol*. 2010;298(3):G375–G383. doi:10.1152/ajpgi.00343.2009

26. Teppola H, Sarkanen JR, Jalonen TO, Linne ML. Morphological differentiation towards neuronal phenotype of SH-SY5Y neuroblastoma cells by estradiol, retinoic acid and cholesterol. *Neurochem Res*. 2016;41(4):731–747. doi:10.1007/s11064-015-1743-6

27. Thiele CJ, Reynolds CP, Israel MA. Decreased expression of N-myc precedes retinoic acid-induced morphological differentiation of human neuroblastoma. *Nature*. 1985;313(6001):404–406. doi:10.1038/313404a0

28. Clagett-Dame M, McNeill EM, Muley PD. Role of all-trans retinoic acid in neurite outgrowth and axonal elongation. *J Neurobiol*. 2006;66(7):739–756. doi:10.1002/neu.20241

29. Shelton MA, Newman JT, Gu H, et al. Loss of microtubule-associated protein 2 immunoreactivity linked to dendritic spine loss in schizophrenia. *Biol Psychiatry*. 2015;78(6):374–385. doi:10.1016/j.biopsych.2014.12.029

30. Constantinescu R, Constantinescu AT, Reichmann H, Janetzky B. Neuronal differentiation and long-term culture of the human neuroblastoma line SH-SY5Y. In: Gerlach M, Deckert J, Double K, Koutsilieri E, eds. *Neuropsychiatric Disorders An Integrative Approach*. Vienna, Austria: Springer Vienna; 2007:17–28. doi:10.1007/978-3-211-73574-9_3

31. Encinas M, Iglesias M, Liu Y, et al. Sequential treatment of SH-SY5Y cells with retinoic acid and brain-derived neurotrophic factor gives rise to fully differentiated, neurotrophic factor-dependent, human neuron-like cells. *J Neurochem*. 2002;75(3):991–1003. doi:10.1046/j.1471-4159.2000.0750991.x

32. Dong R, Yang R, Zhan Y, et al. Single-cell characterization of malignant phenotypes and developmental trajectories of adrenal neuroblastoma. *Cancer Cell*. 2020;38(5):716–733.e6. doi:10.1016/j.ccell.2020.08.014

33. Uchida A, Brown A. Arrival, reversal, and departure of neurofilaments at the tips of growing axons. *Mol Biol Cell*. 2004;15(9):4215–4225. doi:10.1091/mbc.e04-05-0371

34. Scheibe RJ, Ginty DD, Wagner JA. Retinoic acid stimulates the differentiation of PC12 cells that are deficient in cAMP-dependent protein kinase. *J Cell Biol*. 1991;113(5):1173–1182. doi:10.1083/jcb.113.5.1173

35. Murillo JR, Goto-Silva L, Sánchez A, Nogueira FCS, Domont GB, Junqueira M. Quantitative proteomic analysis identifies proteins and pathways related to neuronal development in differentiated SH-SY5Y neuroblastoma cells. *EuPA Open Proteomics*. 2017;16:1–11. doi:10.1016/j.euprot.2017.06.001

36. Wang C, Liu Z, Woo CW, et al. EZH2 mediates epigenetic silencing of neuroblastoma suppressor genes *CASZ1*, *CLU*, *RUNX3*, and *NGFR*. *Cancer Res*. 2012;72(1):315–324. doi:10.1158/0008-5472.CAN-11-0961

37. Simon JA, Lange CA. Roles of the EZH2 histone methyltransferase in cancer epigenetics. *Mutat Res*. 2008;647(1–2):21–29. doi:10.1016/j.mrfmmm.2008.07.010

38. Yin X, Yang S, Zhang M, Yue Y. The role and prospect of JMJD3 in stem cells and cancer. *Biomed Pharmacother*. 2019;118:109384. doi:10.1016/j.biopha.2019.109384